Impact of and correction for instrument sensitivity drift on nanoparticle size measurements by single-particle ICP-MS

Hind El Hadri[a]*, Elijah J. Petersen[b], and Michael R. Winchester[a+]

[a]Chemical Sciences Division, [b]Biosystems and Biomaterials Division, Material Measurement Laboratory, National Institute of Standards and Technology (NIST), 100 Bureau Drive, Gaithersburg, MD 20899

*Present address: Materials Measurement Science Division, Material Measurement Laboratory, National Institute of Standards and Technology (NIST), 100 Bureau Drive, Gaithersburg, MD 20899

[+]Corresponding author e-mail: mrw@nist.gov

Abstract: The effect of ICP-MS instrument sensitivity drift on the accuracy of NP size measurements using single particle (sp)ICP-MS is investigated. Theoretical modeling and experimental measurements of the impact of instrument sensitivity drift are in agreement and indicate that drift can impact the measured size of spherical NPs by up to 25 %. Given this substantial bias in the measured size, a method was developed using an internal standard to correct for the impact of drift and was shown to accurately correct for a decrease in instrument sensitivity of up to 50 % for 30 nm and 60 nm gold nanoparticles.

Keywords: drift correction, gold nanoparticles, instrument sensitivity drift, internal standard, single-particle ICP-MS

1 Introduction

An engineered nanomaterial (ENM) can be defined as a material having any external dimension, internal structure, or surface structure in the nanoscale (approximately 1 nm to 100 nm) and that is designed for a specific purpose or function [1]. The unique and enhanced properties of ENMs compared to traditional materials suggest that they will be used in consumer products increasingly and in more diverse ways in future years. There are many exciting opportunities to employ ENMs in a range of fields, such as composite materials, solar energy, environmental remediation, and aeronautics [2-5]. However, the increased use of ENMs in consumer products and the potential release of ENMs during the product life cycle could have unknown effects on humans and other biological systems, as well as on environmental systems [6-10]. Thus, a substantial research effort is being made to understand the potential environmental, health, and safety (EHS) implications of nanotechnology. One challenging aspect of making measurements for EHS research is the lack of broadly available techniques for accurately and efficiently measuring the size distribution and number concentration of nano-objects (defined as nanomaterials with one, two, or three external dimensions in the nanoscale[1]) in liquid suspension. Techniques such as electron microscopy are time consuming, tedious, and typically require drying the sample prior to analysis, which is a known source of artifacts. Other techniques, such as dynamic light scattering (DLS), are challenged to measure multimodal distributions accurately [11]. NP tracking analysis can overcome the limitations of DLS by detecting small NPs among large ones and determining the number concentration [12], although this method is not element specific and the size distribution of a NP dispersion provided by this technique is sometimes broader than those obtained by other techniques [13]. Nano-objects in suspensions for toxicological tests may undergo changes such as agglomeration/aggregation or dissolution that could lead to inaccurate dosing, if changes to the nano-objects during the test are not measured [14,15].

One technique that shows substantial promise for accurately measuring metal containing nano-objects suspended in liquid solution is single-particle inductively coupled plasma mass spectrometry (spICP-MS). This technique, first developed by Degueldre *et al.*,[16,17] has recently been used to measure gold nanoparticles, silver nanoparticles, zinc oxide nanoparticles, and carbon nanotubes [18-26]. For our purpose, a nanoparticle (NP) is a nano-object for which all three external dimensions are in the nanoscale [27]. Importantly, spICP-MS is sufficiently sensitive to measure nano-objects, including NPs, at environmentally relevant concentrations (parts per trillion mass concentrations). Several factors (e.g., signal dwell time, background correction algorithm, split-particle events, and nebulization transport efficiency) are known to influence the accuracy of spICP-MS measurements [28]. While some strategies to address such factors have been formulated, many improvements remain to be made [29-32]. For example, the split-particle correction approach devised and used in this laboratory has been described in detail [30].

To our knowledge, the impact of drift in the sensitivity of the ICP-MS instrument on spICP-MS analysis has not yet been studied. Drift can be defined as a continuous or incremental change in response of a measuring instrument due to changes in the metrological properties of that measuring instrument [33]. Drift in sensitivity is known to affect the accuracy of ICP-MS analysis generally and can in some cases be quite severe. For example, a previous study from our laboratory showed a spontaneous (i.e., not intentionally introduced) sensitivity drift for the isotope of interest of up to 50 % during a 16 h period while employing a properly functioning instrument [34]. While most ICP-MS

analyses do not require such long operation and sensitivity drift is not often so severe, this observation nonetheless points out that drift can be potentially problematic. Thus, the impact that sensitivity drift could have on spICP-MS measurements could be substantial, but is until now unknown. One option to mitigate the effect of drift during ICP-MS analysis is to include drift correction standards, either a calibration standards or other standards, in the sample run order. However, this approach increases the overall analysis time and does not enable a correction for each individual sample based on the drift at the precise time that sample is being analyzed. Thus, correction for drift in ICP-MS analysis is often performed by the use of an internal standard (ISD). Inclusion of a proper ISD can also help correct for matrix effects. A recent study by Telgmann et al. [23] has used isotope dilution analysis to measure the size distribution of AgNPs spiked with an enriched ^{109}Ag standard. This approach was effective for the correction of matrix effects when testing the AgNPs in complex media such as wastewater and a river water sample. However, the isotope dilution approach is only suitable for NPs composed of a principal element having more than one isotope and for which there exists a readily available isotopically enriched standard. It is not applicable to AuNPs, because Au is monoisotopic.

The aim of this paper is to investigate the potential impact of instrument sensitivity drift on the accuracy of spICP-MS measurements of NP size and size distribution. This investigation was performed both through theoretical modeling and laboratory experiments using National Institute of Standards and Technology (NIST) reference material (RM) gold nanoparticles (AuNPs). To experimentally measure the effect of drift on results in a controlled and quantifiable way, the instrument sensitivity was intentionally decreased after instrument calibration, but prior to spICP-MS analysis of the RM AuNPs. To correct for the significant observed impact of instrument drift, we investigated incorporation of two different ISDs. To our knowledge, this is the first study to correct signal drift induced size bias by incorporation of an ISD.

2 Materials and methods

2.1 Theoretical Modeling of Bias in Measured Diameter of Spherical NPs as a Function of Drift in ICP-MS Instrument Sensitivity

Consider a spICP-MS measurement of NP diameter in a hypothetical suspension of ideal, monodisperse, non-agglomerated, non-aggregated, fully dense, spherical NPs. When the NPs are measured just after instrument calibration and with no change in the ICP-MS instrument sensitivity, let the measured NP mass be m_1, where d_1 is the NP diameter, and ρ is the density:

$$m_1 = \pi \frac{d_1^3}{6} \rho \quad (1)$$

The technique of spICP-MS actually measures the mass of the nanoparticle, from which the diameter is calculated by rearrangement of Eq. 1:

$$d_1 = \sqrt[3]{\frac{6m_1}{\pi\rho}} \quad (2)$$

Now, assume that the same suspension of NPs is measured again after the instrument sensitivity has drifted by a percentage x (e.g., x = - 20 % means that the instrument sensitivity has decreased by 20 %), resulting in a biased NP mass m_2:

$$m_2 = \left(1 + {}^{x}/_{100}\right)m_1 \quad (3)$$

The diameter d_2 calculated from m_2 is then:

$$d_2 = \sqrt[3]{\frac{6m_2}{\pi\rho}} = \sqrt[3]{\frac{6(1+x/100)m_1}{\pi\rho}} \quad (4)$$

Therefore, the percentage y by which the diameter has been biased by the sensitivity drift is:

$$y = 100\left(\frac{d_2}{d_1} - 1\right) = 100\left(\sqrt[3]{1 + \frac{x}{100}} - 1\right) \quad (5)$$

For the example of x = - 20 %, y = - 7 %, meaning that the observed NP diameter theoretically will be biased low by 7 % in the presence of a 20 % reduction in ICP-MS instrument sensitivity that occurs after instrument calibration.

Theoretical modeling of this sort for several other spICP-MS measurements of nano-objects such as cubes, rods, and plates is included in the Electronic Supplementary Material. From those theoretical examples, it is shown that the magnitude of the bias in the measured nano-object dimension(s) induced by instrument sensitivity drift depends on the number of dimensions being measured. Fig S1 in the Electronic Supplementary Material illustrates that the most severe bias occurs for nano-objects having one dimension in the nanoscale (or more precisely, when one dimension of a nano-object is being measured). This is noteworthy, because the equivalent spherical diameter of nanoparticles, which is by far the most common measurement made using spICP-MS, in essence involves all three dimensions.

2.2 Chemicals

Reagent grade high-purity deionized water (minimum resistivity of 18 MΩ cm) obtained from a ModuLab high-flow water purification system (Continental Water Systems, San Antonio, TX, USA) was

used for all sample preparations and dilutions. Concentrated nitric acid (69 % *m*/*m*) and hydrochloric acid (32 % to 38 % *m*/*m*) (Veritas™ double distilled, GFS Chemicals, Columbus, OH, USA) were used in ICP-MS experiments. Gold nanoparticle reference materials with nominal diameters of 30 nm and 60 nm obtained from NIST (RM 8012 and RM 8013, respectively, Gaithersburg, MD, USA) were used in this study. NIST Standard Reference Material® (SRM) 3121 Gold (Au) Standard Solution, SRM 3140 Platinum (Pt) Standard Solution, and SRM 3124a Indium (In) Standard Solution were used to prepare solutions.

2.3 Impact of Instrument Sensitivity Drift on spICP-MS Size Measurements of NIST RM AuNPs

A Thermo XSERIES 7 quadrupole mass spectrometer (Waltham, MA, USA) equipped with a concentric quartz C-Type nebulizer and Ni cones was used throughout this study for spICP-MS measurements. Before analysis, the ICP-MS was tuned using a multi-element standard solution (2 µg L^{-1} of each of Li, Be, Co, In, Ba, Ce and U in 2 % *v*/*v* HNO_3) for maximum ^{115}In sensitivity and minimum oxide ($^{156}CeO/^{140}Ce$) level (< 2 %). Data were collected at *m*/*z* 197 for Au. The sample flow rate was set to 0.6 mL min^{-1} and measured daily in triplicate by weighing the water uptake after 5 min of aspiration.

All samples and working standard solutions were prepared gravimetrically (i.e., on a mass fraction basis). AuNPs were suspended in a solution of deionized water at a particle number concentration between 2.5 x 10^5 g^{-1} and 3.5 x 10^5 g^{-1}. The AuNP stock suspensions were bath sonicated (model 2800, Branson Ultrasonics, Danbury, CT, USA) for 10 min before dilution. Dissolved gold calibration standards were prepared in a range of mass fraction between 0.05 µg L^{-1} and 5 µg L^{-1} either in an aqua regia/thiourea solution (2.0 % *m*/*m* HCl, 0.5 % *m*/*m* HNO_3 and 0.5 % *m*/*m* thiourea) or in deionized water. To test the system repeatability, it was necessary to make several runs of the same sample, and the uptake time was increased (60 s to 120 s) in order to eliminate memory effects and to properly condition the introduction system. Additionally, thoroughly washing the system with 2 % *v*/*v* HNO_3 or aqua regia/thiourea solution was necessary between each sample analysis.

To assess the impact of the instrument sensitivity drift on the accuracy of spICP-MS measurements, the sensitivity of the ICP-MS was intentionally decreased after instrument calibration. Instrument sensitivity was lowered by decreasing the absolute value of the extraction voltage from -600 V to -329 V for a 50 % decrease in the signal intensity. Results were also obtained for a 20 % decrease in the signal intensity through decreasing the detector voltage. The NIST RM AuNPs with nominal sizes of 30 nm and 60 nm were individually analyzed, first without sensitivity reduction and then with the instrument sensitivity decreased by 20 % or 50 %. The time-resolved analysis (TRA) mode of the ICP-MS instrument was used for spICP-MS measurements. Raw data were recorded using Thermo Fisher PlasmaLab software in units of counts per second (cps) and exported into Microsoft Excel for further data processing. AuNP size calculations are described in depth in a later section.

2.4 Use of ISDs to Correct for ICP-MS Instrument Sensitivity Drift

Two elements (In and Pt) were tested as ISDs to correct for the effect of changes in instrument sensitivity on spICP-MS NP size measurements. Indium was tested, because it is widely used as an ISD

for routine ICP-MS analysis. Platinum was also tested, because it has mass-to-charge ratio (*m*/*z* 195) and first ionization energy (8.9587 eV) values close to those of Au (*m*/*z* 197 and 9.2255 eV, respectively). Data were collected at *m*/*z* 197 and *m*/*z* 195 for solutions with Au and Pt, or at *m*/*z* 197 and *m*/*z* 115 for solutions with Au and In.

Because AuNPs were suspended in deionized water, ISDs were also prepared in water and needed to be made freshly before addition to the samples, owing to poor long-term stability of the ISDs in water. ISDs were either directly added to the sample during sample preparation (after dilution) or added on-line using a second peristaltic pump channel and a tee placed directly before sample injection into the nebulizer. The purpose of the tee placed before the nebulizer was to reduce the number of sample preparation steps and to add the ISD immediately before injection, thus decreasing the interaction of the ISD with the AuNPs. When adding the ISDs using the tee, an additional peristaltic pump was used to pump out the waste from the spray chamber. When the ISDs were instead added directly to the sample suspensions, the ISD stocks were first diluted in deionized water and then mixed with 30 nm and 60 nm AuNP samples (diluted in water only) or with dissolved Au solution (diluted in water or in aqua regia/thiourea) to a final ISD concentration of approximately 2 μg L^{-1}.

To assess the impact of the mixing methods on dissolved Au and AuNP measurements, standard solutions of dissolved Au and suspensions of AuNPs were analyzed with introduction of the Pt ISD using the tee or by direct mixing. For these experiments, the dissolved Au standards (0.05 μg L^{-1}, 0.5 μg L^{-1} and 1 μg L^{-1}) were analyzed by ICP-MS using continuous (i.e., not TRA) mode.

The measurement time for spICP-MS analysis was either 100 s or 400 s if one or two isotopes were analyzed, respectively. For most experiments involving the measurement of two isotopes, each dwell time was set to 10 ms, with the quadrupole settling time set to 10 ms between each peak hop. Thus, it was necessary to increase the sample analysis time by a factor of 4 compared to analyzing the AuNPs alone, to allow for the same number of measurement events when analyzing both the ISD and the AuNPs.

2.5 Calculation of AuNP Size

The theoretical equations used in this study are derived from those presented by Pace *et al*.[31] The nanoparticle signal spikes were identified as those with intensities exceeding five times the standard deviation of the background (5σ) [32]. The determination of the mass of the Au nanoparticle m_{Au} causing a signal spike is described by Eq. 6:

$$m_{Au} = \frac{S_{Au}}{slope} \quad (6)$$

where S_{Au} is the background-subtracted intensity of a signal spike and *slope* is the slope of the calibration line generated using dissolved Au solutions. For this purpose, the calibration line is defined using intensity as the ordinate and the mass of Au entering the plasma within a dwell time as the abscissa. The latter, $m_{Au,dwell}$, is given by:

$$m_{Au,dwell} = C_{Au} * t_{dwell} * q_{liq} * \eta_n \quad (7)$$

where C_{Au} is the mass concentration of Au in the given solution being nebulized, t_{dwell} is the dwell time, q_{liq} is the solution nebulization rate, and η_n is the nebulization transport efficiency, which is the fraction of nebulized Au that actually enters the plasma. The nebulization transport efficiency was determined each day by using the particle size method of Pace *et al*.[31] This approach relies on well-characterized reference nanoparticles of a known particle size. Typically, η_n was about 2 %. The use of a tee piece can change the flow rate introduced in the nebulizer and consequently the nebulization efficiency. Nevertheless, the calculations of the size distribution of NPs remain unchanged. Additionally, it has been observed that the sensitivity decrease did not impact the nebulization efficiency. For instance, η_n calculated from the particle frequency was (0.9 ± 0.1) % and (1.0 ± 0.1) % before and after 50 % decrease, respectively.

When using ISD correction, the background-corrected intensity of the ISD S_{ISD} and the mass of the ISD that enters the plasma in a single dwell time $m_{ISD,dwell}$ must be taken into account:

$$m_{Au} = \frac{{}^{S_{Au}}/_{S_{ISD}}}{slope} m_{ISD,dwell} \quad (8)$$

where the slope is determined from the calibration line of dissolved Au (S_{Au}/S_{ISD} as a function of m_{Au}/m_{ISD}). The parameter $m_{ISD,dwell}$ is defined analogously to Eq. 7.

For the data obtained in our study, the ratio of S_{Au} to S_{ISD} cannot be calculated for each individual dwell time window. This is because S_{Au} and S_{ISD} were measured sequentially, not simultaneously, as a result of the instrument peak hopping back and forth between the isotopes. The data stream in TRA mode of S_{Au} and S_{ISD} values was divided into segments for data processing. Each segment contained 100 dwell time windows for S_{Au} and 100 dwell time windows for S_{ISD}. For each segment, S_{ISD} was averaged over the 100 dwell times, and each S_{Au} value in the segment was divided by this average S_{ISD} value. As an example, a dwell time of 10 ms for both ^{197}Au and ^{195}Pt and a total measurement time of 400 s resulted in 200 segments of 2 s each, with each segment containing 100 dwell time windows of the S_{Au} signal. The segment length (100 dwell times) was chosen judiciously to provide some signal averaging (preventing too much noise from the signal fluctuation intrinsically related to the instrument), while avoiding serious depletion of the effectiveness of the ISD to correct for instrument sensitivity drift.

The mean of the size distribution for each run of a given sample suspension was determined as the mean of a Gaussian curve fitted to the histogram using OriginPro 9.1. The uncertainty values given throughout the manuscript are the standard deviations of the Gaussian fitting provided by the OriginPro processing (Gaussian fitting uncertainty). Additionally, estimations of measurement repeatability were determined from at least two replications of each suspension. In this case, the uncertainty was calculated as the standard deviation of the mean of the replicate values.

3 Results and discussion

3.1 Impact of decreased instrument sensitivity on the NP size from theoretical modeling

The dependence of the percentage change in equivalent spherical diameter on the percentage of instrument sensitivity drift is plotted in Fig. 1. Decreases in instrument sensitivity of 20 % and 50 % result in NP diameters that are 7.2 % and 21 % smaller than the actual size, respectively. While it may seem at first glance that the particle size should decrease by 20 % when the instrument sensitivity decreases by that amount, what decreases by 20 % is the measured intensity, which is proportional to the NP mass and to the cube root of the NP diameter. Nevertheless, the impact of instrument sensitivity change on spICP-MS measurements is predicted to substantially impact the results obtained. Sensitivity gains are far less frequent than losses, but are included in the figure for completeness. The case of measuring equivalent spherical diameter depicted in Fig. 1 involves all three external dimensions, because diameter necessarily defines all three dimensions. Theoretical modeling results for several other types of spICP-MS dimensional measurements of nano-objects, along with plots similar to the one shown in Fig. 1 for measurements of two dimensions and one dimension, are given in the Electronic Supplementary Material (see particularly Fig. S1).

Changes of instrument sensitivity of 20 % and 50 % are severe, although they have been observed to occur spontaneously in this laboratory [34]. If the sensitivity drifted by 10 % to 15 %, an amount somewhat regularly observed in our laboratory conducting ICP-MS analysis during an 8 h to 10 h period, this would result in a spICP-MS size bias of approximately 3 % to 5 % for spheres (Fig. 1) and larger biases for other shapes (Electronic Supplementary Material Fig. S1). While other sources of variability and bias in spICP-MS may currently be as or more significant than the bias from instrument drift, correcting for this bias will become increasingly important as the technique matures and other uncertainty sources are accounted for and reduced.

3.2 Impact of instrument sensitivity drift on measured AuNP sizes

The impact of decreased instrument sensitivity, as has been documented to occur during operation of ICP-MS instruments [34], on the calculated AuNP sizes was also experimentally evaluated. The measured equivalent spherical diameters of the NIST 30 nm and 60 nm AuNPs without a change in the instrument sensitivity were (27.6 ± 1.7) nm and (56.2 ± 2.8) nm, respectively (Fig. 2). These uncertainty values account only for the standard deviation of the Gaussian fitting. The average sizes determined by transmission electron microscopy (TEM) and provided in the RM reports of investigation are (27.6 ± 2.1) nm and (56.0 ± 0.5) nm for the nominal 30 nm and 60 nm diameter AuNPs, respectively. The uncertainties for these TEM results are expanded to a level of confidence of approximately 95 % [35,36]. The spICP-MS results are in good agreement with the TEM results.

The impact of sensitivity decreases of 20 % and 50 % on the measured sizes was also evaluated (Fig. 2). For a 20 % decrease in sensitivity, the equivalent spherical diameters of the 30 nm and 60 nm AuNPs were (25.3 ± 1.7) nm and (51.7 ± 2.3) nm, respectively, equivalent to percentage biases of -7.6 %

and -8.4 %, respectively. There was a larger bias in the measured diameters when the sensitivity was decreased by 50 %. Using this condition, the measured sizes were (20.0 ± 2.3) nm and (42.8 ± 3.4) nm for the 30 nm and 60 nm AuNPs, respectively, equivalent to an approximate -25 % bias for both AuNPs. These observed biases are quite close to the theoretically predicted values of -7 % and -21 % for decreases in instrument sensitivity of 20 % and 50 %, respectively, calculated earlier in this paper.

Overall, these data suggest that changes in instrument sensitivity after calibration can substantially impact measured nanoparticle sizes, and that not accounting for changes in sensitivity can lead to biased results. In the subsequent sections, we describe an investigation of the use of ISDs to correct for changes in instrument sensitivity on spICP-MS dimensional measurements.

3.3 Selection and stability of the ISD

When employing an ISD in spICP-MS, it is appropriate for the ISD to be in a stock solution that has a similar matrix to the solution phase of the NP suspensions to be analyzed, because NPs may be unstable relative to changes in solution matrix. The ISD must also be stable in solution both with and without the presence of NPs. For both of these factors, stability should be much more important when the sample suspension and ISD are directly mixed than when mixing via the tee is employed, owing to the much longer contact time between the sample and ISD. Pt and In were each evaluated for use as an ISD applied to spherical diameter measurements of AuNPs.

Indium quickly proved to be unsuitable for this particular application. While this metal is known to be unstable at neutral pH, it was tested nonetheless, because of the possibility that the kinetics of instability would be slow enough to permit its use. However, signal spikes were observed for In in water (Electronic Supplementary Material Fig. S2a), whether it was mixed with AuNPs or not, and for both direct mixing and online ISD introduction using the tee. The signal spikes may be due to formation of indium oxide particles and precipitates [37,38]. Given these findings, use of In as an ISD was abandoned. In contrast to In, Pt provided stable signals (RSD approximately 6 %, Electronic Supplementary Material Fig S2b) in the presence and absence of AuNPs, using both direct mixing and online introduction. Possible explanations for the Pt stability are the formation of hydroxylated species of Pt at neutral pH [39] or sufficiently slow instability kinetics. Because of its superior stability, Pt was utilized as the ISD for the remainder of this study.

3.4 Influence of ICP-MS parameters on AuNP size measurements with Pt internal standardization

The impact of the Pt ISD on the AuNP size measurements in the absence of instrument sensitivity drift was analyzed using different ICP-MS parameters. Results for testing nominal 30 nm and 60 nm NIST RM AuNPs while measuring only Au for an analysis period of 100 s or Au and Pt for a total analysis time of 400 s are presented in Figs. S3a and S3b of the Electronic Supplementary Material. For these measurements, a dwell time of 10 ms for both Au and Pt and a quadrupole settling time of 10 ms were used. The frequencies of AuNP events were equivalent with and without Pt monitoring for both the 30 nm and 60 nm AuNPs. The mean equivalent spherical diameter values for the 30 nm and 60 nm AuNP

distributions were (27.6 ± 1.7) nm and (56.2 ± 2.8) nm, respectively, when an analysis time of 100 s was used and only Au was analyzed. These values are very similar to those measured during a measurement time of 400 s with simultaneous analysis of Pt and Au, (27.2 ± 1.9) nm and (56.1 ± 2.9) nm, respectively. Thus, no significant change in measured size was observed when these two elements were analyzed simultaneously.

The impact of increasing the analysis speed by decreasing the quadrupole settling time from 10 ms to 5 ms or decreasing the dwell time for Pt from 10 ms to 1 ms on the spICP-MS measurement was also assessed. While the results showed that the average signal (in cps) for a dissolved solution of Pt is similar for both dwell times, the RSD of the Pt signal was twice as high for a dwell time of 1 ms (RSD = 12 %) compared to that for a dwell time of 10 ms (RSD = 5.6 %). Thus, in this particular case using a higher dwell time for the ISD improved measurement precision. This finding is expected because the number of ions counted with a dwell time of 1 ms is ten times lower than at 10 ms, and Poisson noise is equal to the square root of the number of ions counted [40]. However, the size of AuNPs determined by this method was not modified given that the S_{ISD} averages were similar; it should be noted that the dwell time for the AuNPs always remained at 10 ms. It might be possible to use shorter dwell times for the ISD without the increased measurement variability by increasing the Pt concentration. However, it is also possible that the increased interactions between Pt and the AuNPs could lead to deleterious effects.

A decrease of the quadrupole settling time from 10 ms to 5 ms did not significantly change the size distribution (Electronic Supplementary Material Fig. S4). The mean sizes for the 30 nm standard were (27.6 ± 2.2) nm and (27.8 ± 2.0) nm for 5 ms and 10 ms settling times, respectively, while the mean sizes for the 60 nm standard were (57.2 ± 3.2) nm and (57.5 ± 3.4) nm, respectively. The small *m*/*z* difference between the Au and Pt isotopes apparently enabled the quadrupole to stabilize adequately with the shorter settling time.

The impact of introduction of the ISD using direct mixing or the tee on the analysis of the dissolved gold and AuNPs was also investigated. The dissolved Au signal decreased by a factor of 1.9 ± 0.1 when the tee was used as compared to the direct mixing approach. This result can be explained by the dilution of the dissolved gold concentration when mixing equivalent volumes of the dissolved gold solution and the ISD solution when using the tee. Indeed, due to a change in the flow rate the nebulization efficiency was modified (from approximately 2 % to about 1 %). Nevertheless, the mean intensity of AuNP spikes (about 8000 cps for 30 nm and 60000 cps for 60 nm AuNPs), and consequently the measured AuNP size, are similar for both ISD introduction approaches as expected.

3.5 Correction of instrument sensitivity drift in AuNP size measurement with use of an ISD

The effectiveness of Pt as an ISD to correct for changes in instrument sensitivity was evaluated. It was important to first assess the impact of ISD correction in the absence of instrument sensitivity drift (i.e., immediately after calibration and without any observable drift). When operating the ICP-MS under this condition, the average size obtained for the 30 nm AuNPs was (27.2 ± 2.0) nm and (27.9 ± 1.9) nm without and with ISD correction, respectively; results obtained for the 30 nm and 60 nm AuNPs without ISD correction are the same as those described in section 3.4 with a measurement time of 400 s and are repeated here to enable a direct comparison to the results with the ISD correction. For the 60 nm AuNPs the average particle size was (56.1 ± 2.9) nm and (55.9 ± 3.1) nm without and with ISD correction,

respectively (see Table 1 and Electronic Supplementary Material Figs. S3b and S3c). Therefore, it is reasonable to conclude that no significantly deleterious effects were observed for the use of Pt as the ISD and the ISD correction.

The size distributions of 30 nm and 60 nm AuNPs after an induced transient 20 % loss of sensitivity were analyzed with and without ISD correction. As shown in Table 1 and described earlier, the mean sizes measured by spICP-MS were underestimated when the ISD was not used, and the relative magnitudes of the underestimations are in agreement with theory. However, when Pt was employed as the ISD, the mean sizes were corrected and in agreement with the expected TEM mean sizes. A more extreme loss of sensitivity of 50 % was also tested by decreasing the extraction voltage; these experiments were conducted by using the tee piece, a modification shown in section 3.4 to not impact spICP-MS results. While a 50 % decrease in sensitivity may seem like an excessive change, instrument drift of this magnitude was observed in a previous study [34]. As shown in Table 1, the results after ISD correction are very similar to those obtained for the 30 nm AuNPs before the instrument sensitivity decrease was induced. The decreased instrument sensitivity caused the mean sizes of the NPs to be underestimated to magnitudes that agree with theoretical modelling results, and use of the ISD effectively corrected the bias. The size distributions for the spICP-MS results for the 30 nm and 60 nm AuNPs on which Table 1 is based are presented in Figs. 3 and 4, respectively.

Some of the newest quadrupole ICP-MS instruments allow one to utilize very short dwell times on the order of microseconds, with quadrupole settling times that can also be very short or even omitted. With such capabilities, the method developed in this study could be applied using an almost simultaneous ratio of analyte and internal standard signal intensities during the analysis of individual nanoparticles, producing results that might be more accurate. As a way to simulate crudely this type of capability, the results in Fig. 3 were recalculated without averaging the Pt signal over 100 dwell time windows, as described in section 2.5, but by pairing each individual Pt intensity measurement with its adjoining Au intensity measurement (Electronic Supplementary Material Fig. S5). When visually compared, the results computed in this way do not seem to be better than those in Fig. 3. As noted, however, this is a crude simulation at best, and actual tests on an instrument with the advanced capabilities will need to be performed at a later date. Interestingly, an instrument capable of conducting rapid peak hopping opens the possibility of performing multielement analyses on single nanoparticles, which was impossible with quadrupoles only a few years ago.

Of course, essentially truly simultaneous measurements of multiple isotopes are possible with ICP-MS technologies that do not employ quadrupoles, and the ISD approach demonstrated here could certainly be applied. However, each alternative has disadvantages. Time-of-flight (TOF) instruments have been utilized for simultaneous, multielement analyses for many years, but these instruments generally have relatively poor sensitivity and limits of detection (LODs). Multicollector instruments offer very good sensitivity and LODs, but are extremely expensive and are constrained in the range of mass-to-charge ratios that can be monitored in a single experiment, thereby limiting the possible choices of internal standard.

It would, in theory, be possible to correct for instrument drift using enriched isotope standards of the same element, an approach that was previously used to correct matrix effects in analyses of AgNPs [23]. However, this approach is impossible when the analyte is monoisotopic or when a suitable isotopically enriched standard is unavailable.

For the study reported in this paper, AuNPs were selected as a suitable test case. The approach described for drift correction obviously should be applicable to spICP-MS analyses of NPs other than AuNPs. In any case it is important to conduct preliminary experiments as described above for Pt with AuNPs to assess the necessary quadrupole settling time, variability in the ISD signal, and stability of the ISD in the matrix.

4 Conclusions

The study described in this paper shows clearly that a change in ICP-MS instrument sensitivity after calibration can induce bias in the measured NP size distributions and in the mean sizes derived from those distributions. It also demonstrates effective correction of this bias through the use of a well-chosen ISD. The size distribution calculation relies on a calibration curve obtained after analysis of dissolved Au standards [31] with incorporation of the ISD and before any significant change in sensitivity. Therefore, while the average AuNP size measured without the ISD was biased by the change in the instrument sensitivity, the concomitant change in the ISD signal intensity could be used to correct for the instrument sensitivity loss. The ISD can also help to correct for matrix effects, which are of particular interest when analyzing complex samples (environmental or biological) and when calibrating using calibrants that have a matrix that is not precisely the same as the matrix of the unknown sample. One limitation of the use of an ISD is that split-pulse correction, as devised and implemented in this laboratory [30], is not possible, because two consecutive pulses in the data set do not correspond to two consecutive time periods in the analysis. Recent innovations in spICP-MS equipment (e.g., quadrupole instruments with very short dwell time and rapid peak hopping capabilities [41] and ICP-TOF-MS [42]) are much less prone to measurement bias induced by split particle events.

Electronic Supplementary Material Available

Theoretical modeling of the impact of instrument sensitivity drift on sp-ICP-MS measurements of the dimension(s) of nano-objects, and figures showing the theoretical bias caused by instrument drift for nano-objects with different numbers of dimensions, ICP-MS intensity of indium in an aqueous solution without nanoparticles, impact of different analysis times with and without using Pt as an internal standard for correction on AuNP size distributions, and the impact of quadrupole settling time on AuNP size distributions.

NIST Disclaimer

The identification of any commercial product or trade name does not imply endorsement or recommendation by the National Institute of Standards and Technology, nor does it imply that it is necessarily the best available for the purpose.

Compliance With Ethical Standards

Conflict of interest The authors declare that they have no conflict of interest.

References

1. ISO/TS 80004-1:2010 Nanotechnologies – Vocabulary - Part 1: Core Terms (2010). International Organization for Standardization, Geneva, Switzerland

2. Lee J, Mahendra S, Alvarez PJJ (2010) Nanomaterials in the Construction Industry: A Review of Their Applications and Environmental Health and Safety Considerations. ACS Nano 4 (7):3580-3590. doi:10.1021/nn100866w

3. Bauer F, Flyunt R, Czihal K, Ernst H, Naumov S, Buchmeiser MR (2007) UV curing of nanoparticle reinforced acrylates. Nuclear Instruments and Methods in Physics Research Section B: Beam Interactions with Materials and Atoms 265 (1):87-91. doi:http://dx.doi.org/10.1016/j.nimb.2007.08.030

4. Kamat PV (2012) Boosting the Efficiency of Quantum Dot Sensitized Solar Cells through Modulation of Interfacial Charge Transfer. Accounts of Chemical Research 45 (11):1906-1915. doi:10.1021/ar200315d

5. Petersen EJ, Pinto RA, Shi X, Huang Q (2012) Impact of size and sorption on degradation of trichloroethylene and polychlorinated biphenyls by nano-scale zerovalent iron. Journal of Hazardous Materials 243 (0):73-79. doi:http://dx.doi.org/10.1016/j.jhazmat.2012.09.070

6. Klaine SJ, Koelmans AA, Horne N, Carley S, Handy RD, Kapustka L, Nowack B, von der Kammer F (2012) Paradigms to assess the environmental impact of manufactured nanomaterials. Environmental Toxicology and Chemistry 31 (1):3-14. doi:10.1002/etc.733

7. Nowack B, Ranville JF, Diamond S, Gallego-Urrea JA, Metcalfe C, Rose J, Horne N, Koelmans AA, Klaine SJ (2012) Potential scenarios for nanomaterial release and subsequent alteration in the environment. Environmental Toxicology and Chemistry 31 (1):50-59. doi:10.1002/etc.726

8. Oomen AG, Bos PMJ, Fernandes TF, Hund-Rinke K, Boraschi D, Byrne HJ, Aschberger K, Gottardo S, von der Kammer F, Kühnel D, Hristozov D, Marcomini A, Migliore L, Scott-Fordsmand J, Wick P, Landsiedel R (2014) Concern-driven integrated approaches to nanomaterial testing and assessment – report of the NanoSafety Cluster Working Group 10. Nanotoxicology 8 (3):334-348. doi:doi:10.3109/17435390.2013.802387

9. Petersen EJ, Zhang L, Mattison NT, O'Carroll DM, Whelton AJ, Uddin N, Nguyen T, Huang Q, Henry TB, Holbrook RD, Chen KL (2011) Potential Release Pathways, Environmental Fate, And Ecological Risks of Carbon Nanotubes. Environmental Science & Technology 45 (23):9837-9856. doi:10.1021/es201579y

10. Krug HF, Wick P (2011) Nanotoxicology: An Interdisciplinary Challenge. Angewandte Chemie International Edition 50 (6):1260-1278. doi:10.1002/anie.201001037

11. Hassellöv M, Readman J, Ranville J, Tiede K (2008) Nanoparticle analysis and characterization methodologies in environmental risk assessment of engineered nanoparticles. Ecotoxicology 17 (5):344-361. doi:10.1007/s10646-008-0225-x

12. Gallego-Urrea JA, Tuoriniemi J, Hassellöv M (2011) Applications of particle-tracking analysis to the determination of size distributions and concentrations of nanoparticles in environmental, biological and food samples. TrAC Trends in Analytical Chemistry 30 (3):473-483. doi:http://dx.doi.org/10.1016/j.trac.2011.01.005

13. Pace HE, Rogers NJ, Jarolimek C, Coleman VA, Gray EP, Higgins CP, Ranville JF (2012) Single Particle Inductively Coupled Plasma-Mass Spectrometry: A Performance Evaluation and Method Comparison in the Determination of Nanoparticle Size. Environmental Science & Technology 46 (22):12272-12280. doi:10.1021/es301787d

14. Petersen EJ, Henry TB, Zhao J, MacCuspie RI, Kirschling TL, Dobrovolskaia MA, Hackley V, Xing B, White JC (2014) Identification and Avoidance of Potential Artifacts and Misinterpretations in Nanomaterial Ecotoxicity Measurements. Environmental Science & Technology 48 (8):4226-4246. doi:10.1021/es4052999

15. Petersen EJ, Diamond SA, Kennedy AJ, Goss GG, Ho K, Lead J, Hanna SK, Hartmann NB, Hund-Rinke K, Mader B, Manier N, Pandard P, Salinas ER, Sayre P (2015) Adapting OECD Aquatic Toxicity Tests for Use with Manufactured Nanomaterials: Key Issues and Consensus Recommendations. Environmental Science & Technology 49 (16):9532-9547. doi:10.1021/acs.est.5b00997

16. Degueldre C, Favarger PY (2003) Colloid analysis by single particle inductively coupled plasma-mass spectroscopy: a feasibility study. Colloids and Surfaces A: Physicochemical and Engineering Aspects 217 (1–3):137-142. doi:http://dx.doi.org/10.1016/S0927-7757(02)00568-X

17. Degueldre C, Favarger PY, Bitea C (2004) Zirconia colloid analysis by single particle inductively coupled plasma–mass spectrometry. Analytica Chimica Acta 518 (1–2):137-142. doi:http://dx.doi.org/10.1016/j.aca.2004.04.015

18. Reed RB, Goodwin DG, Marsh KL, Capracotta SS, Higgins CP, Fairbrother DH, Ranville JF (2013) Detection of single walled carbon nanotubes by monitoring embedded metals. Environmental Science: Processes & Impacts 15 (1):204-213. doi:10.1039/C2EM30717K

19. Mitrano DM, Lesher EK, Bednar A, Monserud J, Higgins CP, Ranville JF (2012) Detecting nanoparticulate silver using single-particle inductively coupled plasma–mass spectrometry. Environmental Toxicology and Chemistry 31 (1):115-121. doi:10.1002/etc.719

20. Degueldre C, Favarger PY, Wold S (2006) Gold colloid analysis by inductively coupled plasma-mass spectrometry in a single particle mode. Analytica Chimica Acta 555 (2):263-268. doi:http://dx.doi.org/10.1016/j.aca.2005.09.021

21. Gray EP, Coleman JG, Bednar AJ, Kennedy AJ, Ranville JF, Higgins CP (2013) Extraction and Analysis of Silver and Gold Nanoparticles from Biological Tissues Using Single Particle Inductively Coupled Plasma Mass Spectrometry. Environmental Science & Technology 47 (24):14315-14323. doi:10.1021/es403558c

22. Laborda F, Bolea E, Jiménez-Lamana J (2013) Single Particle Inductively Coupled Plasma Mass Spectrometry: A Powerful Tool for Nanoanalysis. Analytical Chemistry 86 (5):2270-2278. doi:10.1021/ac402980q

23. Telgmann L, Metcalfe CD, Hintelmann H (2014) Rapid size characterization of silver nanoparticles by single particle ICP-MS and isotope dilution. Journal of Analytical Atomic Spectrometry 29 (7):1265-1272. doi:10.1039/C4JA00115J

24. Peters RB, Rivera Z, van Bemmel G, Marvin HP, Weigel S, Bouwmeester H (2014) Development and validation of single particle ICP-MS for sizing and quantitative determination of nano-silver in chicken meat. Anal Bioanal Chem 406 (16):3875-3885. doi:10.1007/s00216-013-7571-0

25. Hineman A, Stephan C (2014) Effect of dwell time on single particle inductively coupled plasma mass spectrometry data acquisition quality. Journal of Analytical Atomic Spectrometry 29 (7):1252-1257. doi:10.1039/C4JA00097H

26. Linsinger TJ, Peters R, Weigel S (2014) International interlaboratory study for sizing and quantification of Ag nanoparticles in food simulants by single-particle ICPMS. Anal Bioanal Chem 406 (16):3835-3843. doi:10.1007/s00216-013-7559-9

27. Liber K, Doig LE, White-Sobey SL (2011) Toxicity of uranium, molybdenum, nickel, and arsenic to Hyalella azteca and Chironomus dilutus in water-only and spiked-sediment toxicity tests. Ecotoxicol Environ Saf 74 (5):1171-1179. doi:10.1016/j.ecoenv.2011.02.014

28. Montoro Bustos AR, Petersen EJ, Possolo A, Winchester MR (2015) Post hoc Interlaboratory Comparison of Single Particle ICP-MS Size Measurements of NIST Gold Nanoparticle Reference Materials. Analytical Chemistry 87 (17):8809-8817. doi:10.1021/acs.analchem.5b01741

29. Laborda F, Jimenez-Lamana J, Bolea E, Castillo JR (2013) Critical considerations for the determination of nanoparticle number concentrations, size and number size distributions by single particle ICP-MS. Journal of Analytical Atomic Spectrometry 28 (8):1220-1232. doi:10.1039/C3JA50100K

30. Liu J, Murphy KE, MacCuspie RI, Winchester MR (2014) Capabilities of Single Particle Inductively Coupled Plasma Mass Spectrometry for the Size Measurement of Nanoparticles: A Case Study on Gold Nanoparticles. Analytical Chemistry 86 (7):3405-3414. doi:10.1021/ac403775a

31. Pace HE, Rogers NJ, Jarolimek C, Coleman VA, Higgins CP, Ranville JF (2011) Determining Transport Efficiency for the Purpose of Counting and Sizing Nanoparticles via Single Particle Inductively Coupled Plasma Mass Spectrometry. Analytical Chemistry 83 (24):9361-9369. doi:10.1021/ac201952t

32. Tuoriniemi J, Cornelis G, Hassellöv M (2012) Size Discrimination and Detection Capabilities of Single-Particle ICPMS for Environmental Analysis of Silver Nanoparticles. Analytical Chemistry 84 (9):3965-3972. doi:10.1021/ac203005r

33. ISO (2008) International Vocabulary of Basic and General Terms in Metrology - Basic and general concepts and associated terms (VIM), 3rd edition.108

34. Turk GC, Yu LL, Salit ML, Guthrie WF (2001) Using inductively coupled plasma–mass spectrometry for calibration transfer between environmental CRMs. Fresenius J Anal Chem 370 (2-3):259-263. doi:10.1007/s002160100790

35. NIST (2012) Reference Material® 8012 Gold Nanoparticles, Nominal 30 nm Diameter. National Institut of Standards and Technology,

36. NIST (2012) Reference Material® 8013 Gold Nanoparticles, Nominal 60 nm Diameter. National Institut of Standards and Technology,

37. Moeller T (1941) Contributions to the Chemistry of Indium. III. An Electrometric Study of the Precipitation of Hydrous Indium Hydroxide1. Journal of the American Chemical Society 63 (10):2625-2628. doi:10.1021/ja01855a026

38. Busev AI (2013) The Analytical Chemistry of Indium: International Series of Monographs on Analytical Chemistry. Elsevier Science,

559 39. Azaroual M, Romand B, Freyssinet P, Disnar J-R (2001) Solubility of platinum in aqueous solutions at
560 25°C and pHs 4 to 10 under oxidizing conditions. Geochimica et Cosmochimica Acta 65 (24):4453-4466.
561 doi:http://dx.doi.org/10.1016/S0016-7037(01)00752-9

562 40. Laborda F, Medrano J, Castillo JR (2001) Quality of quantitative and semiquantitative results in
563 inductively coupled plasma mass spectrometry. Journal of Analytical Atomic Spectrometry 16 (7):732-
564 738. doi:10.1039/B101814K

565 41. Montano MD, Badiei HR, Bazargan S, Ranville JF (2014) Improvements in the detection and
566 characterization of engineered nanoparticles using spICP-MS with microsecond dwell times.
567 Environmental Science: Nano 1 (4):338-346. doi:10.1039/C4EN00058G

568 42. Borovinskaya O, Gschwind S, Hattendorf B, Tanner M, Günther D (2014) Simultaneous Mass
569 Quantification of Nanoparticles of Different Composition in a Mixture by Microdroplet Generator-
570 ICPTOFMS. Analytical Chemistry 86 (16):8142-8148. doi:10.1021/ac501150c

571

572

Figure captions

Fig. 1: Theoretical change in the equivalent spherical diameter of nanoparticles measured by spICP-MS caused by drift in the sensitivity of the instrument

Fig. 2: Size distributions of AuNPs with nominal diameters of a) 30 nm and b) 60 nm measured by spICP-MS under normal operating conditions, with a 20 % loss of sensitivity, and with a 50 % loss of sensitivity (at least two replicates were combined for each histogram)

Fig. 3: Size distributions of AuNPs with nominal diameters of a) 30 nm and b) 60 nm in the absence of instrument sensitivity drift and with and without ISD correction after a sensitivity decrease of 20 %. Duplicate replicates were combined for each histogram. The measurement time was 400 s; dwell times were 10 ms for both Au and Pt; quadrupole settling time was 10 ms. For the "No decrease" data the samples were analyzed just before the loss of sensitivity was induced. Pt was added directly into the sample solution before analysis.

Fig. 4: Size distributions of AuNPs with nominal diameters of a) 30 nm and b) 60 nm in the absence of instrument sensitivity drift and with and without ISD correction after a sensitivity decrease of 50 %. Triplicate replicates were combined for each histogram. The measurement time was 200 s; dwell times were 10 ms for Au and 1 ms for Pt; quadrupole settling time was 10 ms. For the "No decrease" data, the samples were analyzed just before the loss of sensitivity was induced. Pt was added with the tee.

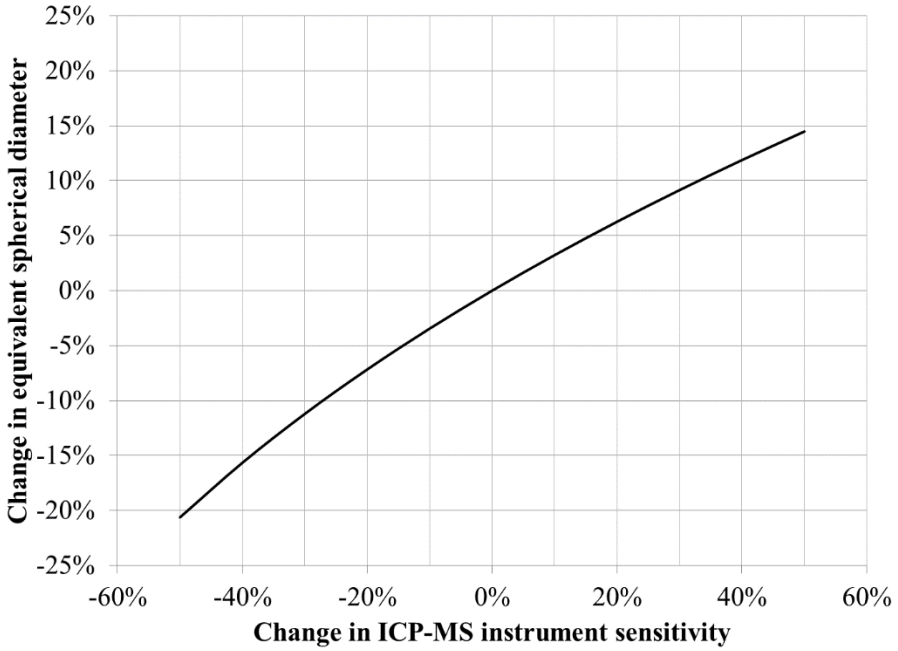

595

596 Fig. 1: Theoretical change in the equivalent spherical diameter of nanoparticles measured by
597 spICP-MS caused by drift in the sensitivity of the instrument

598

599

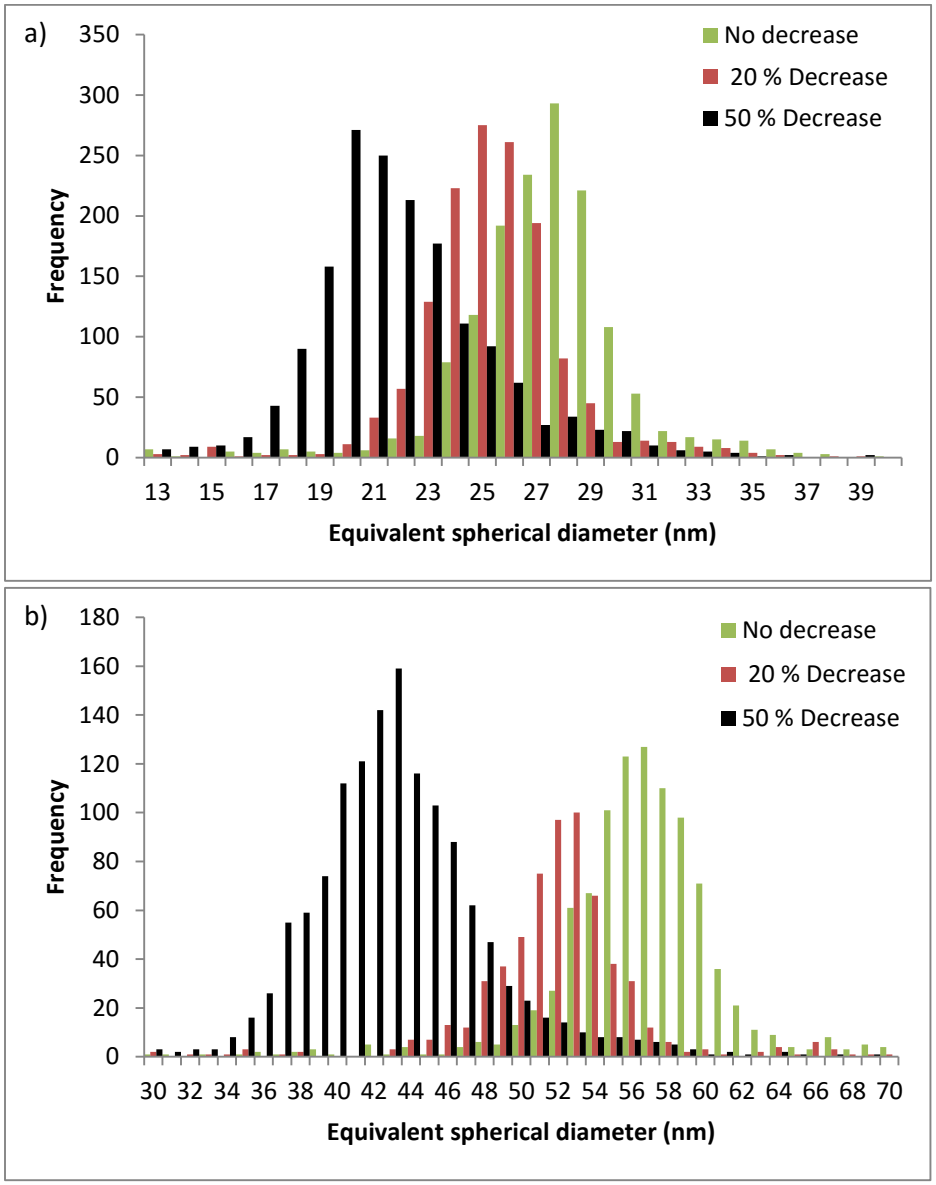

Fig. 2: Size distributions of AuNPs with nominal diameters of a) 30 nm and b) 60 nm measured by spICP-MS under normal operating conditions, with a 20 % loss of sensitivity, and with a 50 % loss of sensitivity (at least two replicates were combined for each histogram)

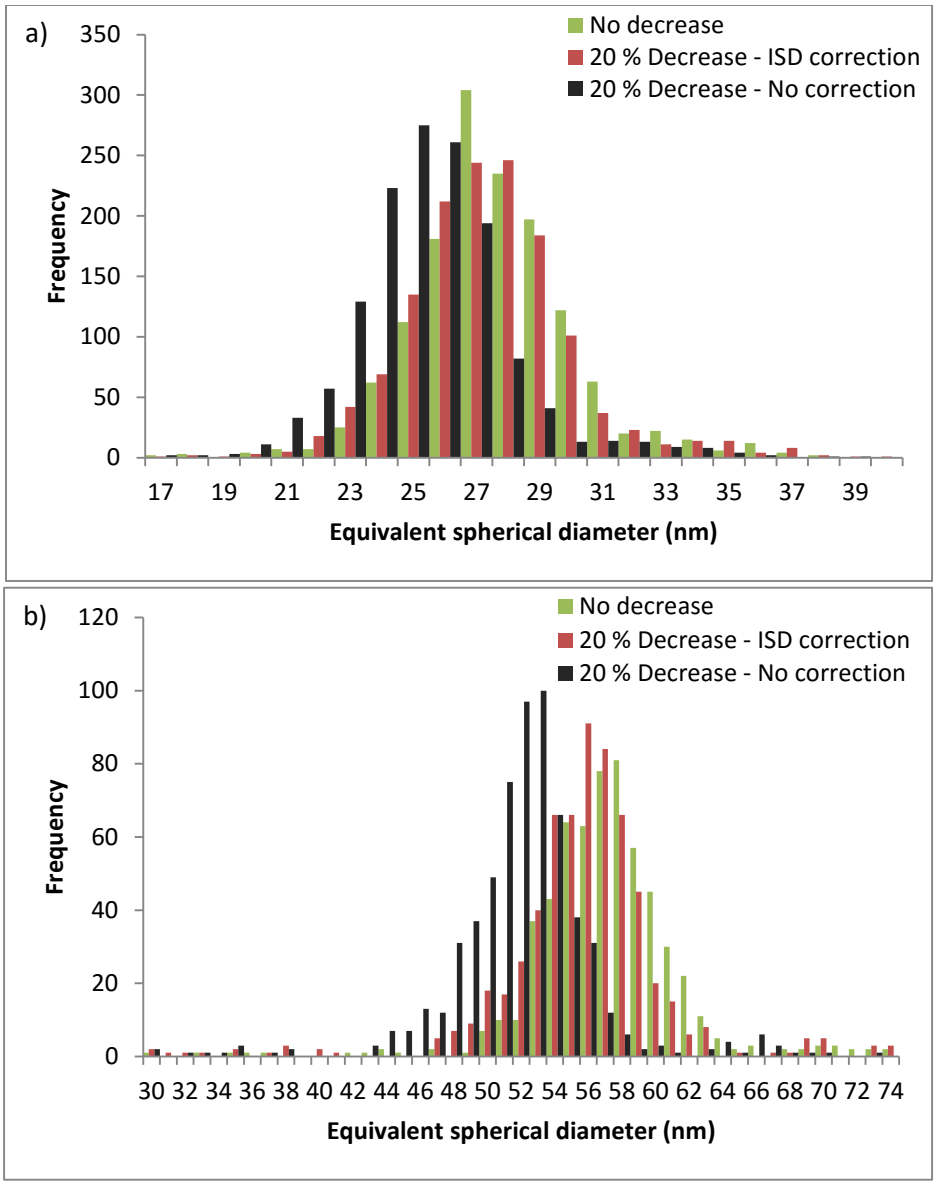

608

609

610 **Fig. 3**: Size distributions of AuNPs with nominal diameters of a) 30 nm and b) 60 nm in the
611 absence of instrument sensitivity drift and with and without ISD correction after a sensitivity
612 decrease of 20 %. Duplicate replicates were combined for each histogram. The measurement time
613 was 400 s; dwell times were 10 ms for both Au and Pt; quadrupole settling time was 10 ms. For
614 the "No decrease" data the samples were analyzed just before the loss of sensitivity was induced.
615 Pt was added directly into the sample solution before analysis

616

617

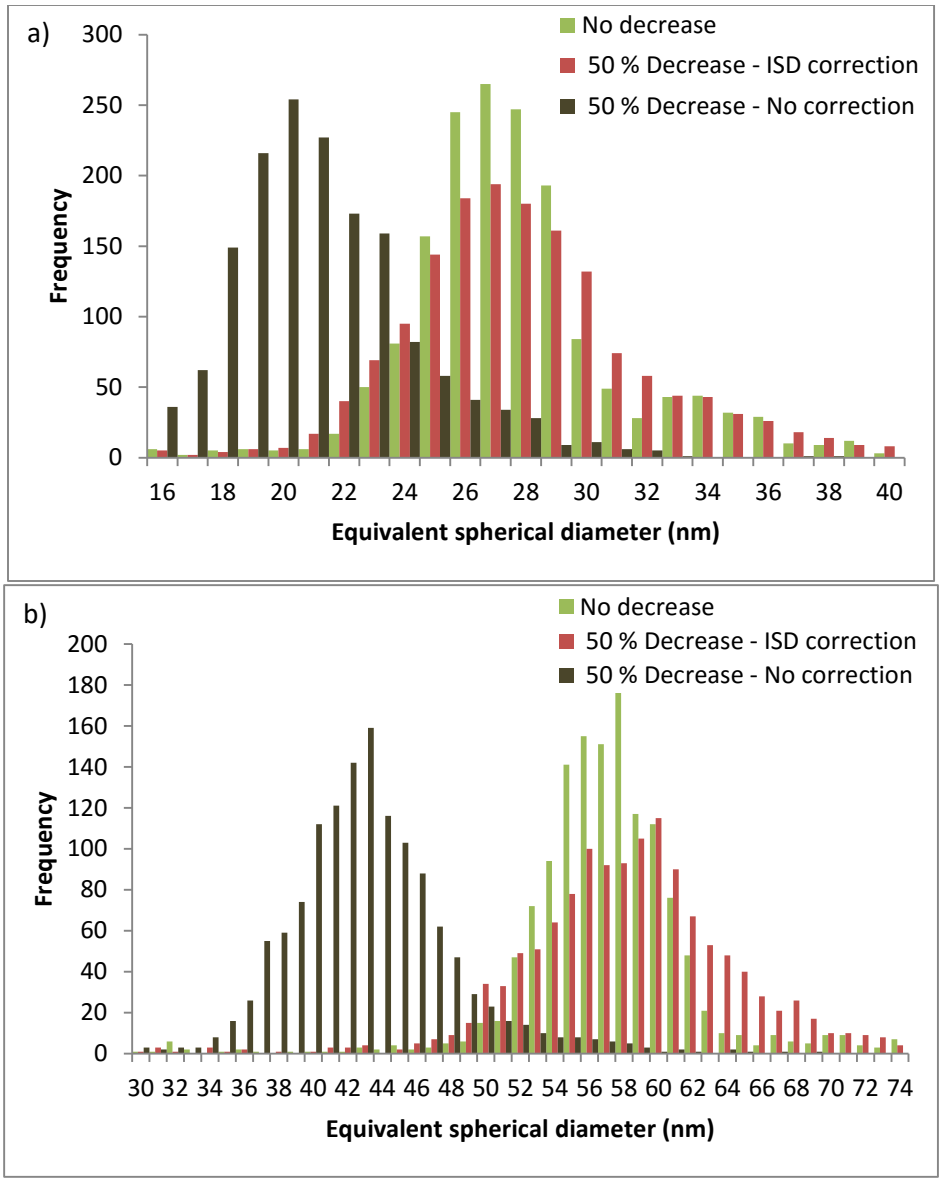

Fig. 4: Size distributions of AuNPs with nominal diameters of a) 30 nm and b) 60 nm in the absence of instrument sensitivity drift and with and without ISD correction after a sensitivity decrease of 50 %. Triplicate replicates were combined for each histogram. The measurement time was 200 s; dwell times were 10 ms for Au and 1 ms for Pt; quadrupole settling time was 10 ms. For the "No decrease" data, the samples were analyzed just before the loss of sensitivity was induced. Pt was added with the tee.

Table 1: Impact of ICP-MS instrument sensitivity drift on NP size measured with spICP-MS, and correction of the effect using Pt as an ISD

			Uncertainty of the Gaussian fitting		spICP-MS repeatability Mean Size (nm)[a]		Bias in Mean Size Without ISD	
AuNPs	TEM Mean Size (nm)[b]	Sensitivity Decrease[c]	With Pt ISD	Without Pt ISD	With Pt ISD	Without Pt ISD	Experimental[d]	Theoretical[e]
RM 8012	27.6 ± 2.1	0 %	27.9 ± 1.9	27.2 ± 2.0	27.9 ± 0.1	27.1 ± 0.2	---	---
		- 20 %	27.5 ± 1.9	25.3 ± 1.7	27.3 ± 0.4	25.4 ± 0.2	- 6.8 %	- 7.2 %
		- 50 %	27.5 ± 3.0	20.0 ± 2.3	27.3 ± 0.2	20.6 ± 0.6	- 25 %	- 21 %
RM 8013	56.0 ± 0.5	0 %	55.9 ± 3.1	56.1 ± 2.9	56.2 ± 0.3	56.0 ± 0.2	---	---
		- 20 %	55.7 ± 2.5	51.7 ± 2.3	56.1 ± 0.6	52.2 ± 0.7	- 6.9 %	- 7.2 %
		- 50 %	57.6 ± 4.5	42.8 ± 3.4	58.3 ± 1.4	42.6 ± 0.9	- 27 %	- 21 %

[a] Average of means of Gaussian fits to 2 or 3 individual data sets obtained by replicate runs of the same sample. Uncertainty is one standard deviation of the 2 or 3 values. Therefore, only measurement repeatability is taken into account.

[b] From NIST Report of Investigation. Uncertainty is expanded to a level of confidence of approximately 95 %, but includes only measurement repeatability.

[c] Obtained by decreasing absolute values of the extraction voltage for 50 % decrease and detector voltage for 20 % decrease.

[d] Relative difference between spICP-MS mean sizes with and without use of Pt ISD.

[e] See Fig. 1.